

Double-Higgs boson production in the high-energy limit: planar master integrals

Joshua Davies^a, Go Mishima^{a,b}, Matthias Steinhauser^a, David Wellmann^a

^a*Institut für Theoretische Teilchenphysik
Karlsruhe Institute of Technology (KIT)
76128 Karlsruhe, Germany*

^b*Institut für Kernphysik
Karlsruhe Institute of Technology (KIT)
76344 Eggenstein-Leopoldshafen, Germany*

Abstract

We consider the virtual corrections to the process $gg \rightarrow HH$ at NLO in the high energy limit and compute the corresponding planar master integrals in an expansion for small top quark mass. We provide details on the evaluation of the boundary conditions and present analytic results expressed in terms of harmonic polylogarithms.

1 Introduction

One of the main aims of particle physics in the coming years is the exploration of the scalar sector of the theory which describes fundamental interactions, be it the Standard Model or an extension. One has to clarify whether the Higgs boson is a fundamental particle and how the particles of the theory obtain their mass. A process which helps to find answers to these questions is the production of Higgs boson pairs, since it is the simplest process which is sensitive to the triple-Higgs boson coupling. Although experimentally quite challenging, there is a chance that double Higgs production will be observed after the the high-luminosity upgrade of the CERN LHC.

The leading order (LO) corrections to Higgs boson pair production have been computed in Refs. [1, 2] including the exact dependence on the top quark mass and the Mandelstam variables. At next-to-leading order (NLO), QCD corrections were computed for the first time in Ref. [3] in the infinite top quark mass limit using an effective theory and an independent cross check was provided in [4] by performing an asymptotic expansion in the full theory. In this way a quantitative estimate of the quark mass effects could be provided. Virtual NLO corrections in the large- m_t limit have also been computed in Ref. [5], confirming the results of Ref. [4]. Finite top quark mass effects have also been considered in Ref. [6], in which the exact real radiation contribution is combined with the effective-theory virtual corrections. Within the effective theory also next-to-next-to-leading (NNLO) contributions are available [7, 8]. The NNLO result was completed in Ref. [9] in which the three-loop matching coefficient of the effective operator for two Higgs bosons and two, three or four gluons was computed. Note that it differs from that of single Higgs boson production. The result of [9] has been complemented by power-suppressed terms in the top quark mass in Ref. [10], where the soft-virtual approximation was constructed. The resummation of threshold-enhanced logarithms to next-to-next-to-leading logarithmic (NNLL) accuracy has been performed in Refs. [11, 12] and transverse momentum resummation has been considered in Ref. [13]. Differential distributions through NNLO for various observables were computed in Ref. [14] in the heavy-top limit. Finally, exact NLO results became available in Refs. [15, 16] using a numerical approach for the computation of the two-loop virtual corrections. More recently these results have been matched to parton showers in Ref. [17].

In this paper we study a class of massive two-loop four-point functions with massless external particles. We describe in detail the methods used for the computation of the amplitudes and in particular the evaluation of the master integrals. We aim to study double Higgs boson production via the process $gg \rightarrow HH$. Numerical NLO results are available [15, 16], however the calculation of cross sections is computationally expensive and we want to provide an independent cross check in the high-energy region. We wish to provide results in terms of compact analytic expressions which can be used to construct simple approximations or can be used directly in the kinematic region in which they are valid. In this paper we provide the first step towards this goal by considering the part of the amplitude which is expressed in terms of planar master integrals.

We perform our calculation in the limit of vanishing Higgs boson mass which provides, as we will demonstrate in Section 3, a good approximation to the general case where $m_H \neq 0$. Furthermore, finite Higgs-mass effects can be incorporated by a simple Taylor expansion. Recently the amplitudes for single-Higgs boson plus jet production have been considered in the limit of large Higgs transverse momentum [18]. In this reference an expansion for small Higgs boson mass has been performed and thus the underlying integrals are the same as those of our calculation, so part of our findings can be cross checked against Ref. [18].

In the recent literature one can find several calculations where two-loop box integrals are also involved. However, the underlying integral families and/or the kinematics of the external and internal masses are different. For example, in Ref. [19] the amplitude of a Higgs boson and three partons has been considered. In the limit $m_H \rightarrow 0$ their integrals are also the same as ours. However, this limit cannot be taken since the calculation is performed in the Euclidean region with the assumption $m_H^2 < s < 0$ and the results are expressed in terms of multiple polylogarithms, which can not easily be analytically continued into other regions. Similar arguments apply to other recent calculations such as [20] or [21]; analytic results have been obtained in terms of multiple polylogarithms which can in principle be evaluated numerically, but are very unwieldy. This is another reason why we have decided to perform an expansion in the high energy limit. Our final results have a simple structure in terms of harmonic polylogarithms and can be evaluated numerically in a fast and reliable manner.

An interesting approach to obtain simple and easy-to-evaluate expressions for $gg \rightarrow HH$ at NLO has been developed in Ref. [22] where the large top mass expansion has been combined with expansion terms obtained for the top threshold. A good approximation of the exact (purely numerical) result [15, 16] has been constructed by combining the different kinematic regions using Padé approximants. Further improvement is expected after incorporating information about the $gg \rightarrow HH$ amplitude at high energies which is the main purpose of this work.

The remainder of the paper is organized as follows: we introduce our notation in Section 2. In Section 3 we briefly consider the one-loop corrections to $gg \rightarrow HH$ in the high-energy limit to provide motivation for our calculation, and Section 4 describes the reduction of the amplitude to master integrals. The main part of the paper is Section 5 in which we discuss the calculation of the master integrals. We describe in detail the method we used to compute the boundary values necessary for the solution of differential equations for the master integrals. In this paper we refrain from presenting long formulae, which instead can be found in the ancillary file of this paper [23].

2 $gg \rightarrow HH$ amplitude and kinematics

The amplitude $g(q_1)g(q_2) \rightarrow H(q_3)H(q_4)$, where all momenta are incoming, is conveniently described in terms of the following variables

$$s = (q_1 + q_2)^2, \quad t = (q_1 + q_3)^2, \quad u = (q_2 + q_3)^2, \quad (1)$$

where we have that

$$q_1^2 = q_2^2 = 0, \quad q_3^2 = q_4^2 = m_H^2, \quad s + t + u = 2m_H^2. \quad (2)$$

Here we make the approximation $m_H = 0$ which significantly simplifies the two-loop calculation. Then we have instead that

$$s = 2q_1 \cdot q_2, \quad t = 2q_1 \cdot q_3, \quad u = 2q_2 \cdot q_3 = -s - t, \quad (3)$$

and integrals will depend on the variables s, t, m_t^2 . Note that finite Higgs mass effects can be implemented by a simple Taylor expansion. Each integral is proportional to $s^{a_1}(s/\mu^2)^{-\epsilon a_2}$ where $a_2 = 1(2)$ at one-(two-)loop order, a_1 is its overall mass dimension, μ is the renormalization scale and we work in $d = 4 - 2\epsilon$ dimensions. In our calculation of the master integrals we expand the integrals for small top quark mass. Thus, effectively we assume that $m_t^2 \ll s, t$.

Due to Lorentz and gauge invariance there are only two independent Lorentz structures and we can write

$$\mathcal{M} = \varepsilon_{1,\mu}\varepsilon_{2,\nu}\mathcal{M}^{\mu\nu} = \varepsilon_{1,\mu}\varepsilon_{2,\nu}(\mathcal{M}_1 A_1^{\mu\nu} + \mathcal{M}_2 A_2^{\mu\nu}), \quad (4)$$

where

$$\begin{aligned} A_1^{\mu\nu} &= g^{\mu\nu} - \frac{1}{q_{12}}q_1^\nu q_1^\mu, \\ A_2^{\mu\nu} &= g^{\mu\nu} + \frac{q_{33}}{q_T^2 q_{12}}q_1^\nu q_2^\mu - \frac{2q_{23}}{q_T^2 q_{12}}q_1^\nu q_3^\mu - \frac{2q_{13}}{q_T^2 q_{12}}q_3^\nu q_2^\mu + \frac{2}{q_T^2}q_3^\mu q_3^\nu, \end{aligned} \quad (5)$$

and

$$q_{ij} = q_i \cdot q_j, \quad q_T^2 = \frac{2q_{13}q_{23}}{q_{12}} - q_{33}. \quad (6)$$

The projectors to obtain \mathcal{M}_1 and \mathcal{M}_2 from $\mathcal{M}^{\mu\nu}$ via the relation

$$\mathcal{M}_i = P_{i,\mu\nu}\mathcal{M}^{\mu\nu} \quad (7)$$

are given by (see also, e.g., Ref. [15])

$$P_{1,\mu\nu} = -\frac{q_{1,\nu}q_{2,\mu}q_{33}}{4q_{12}q_T^2} - \frac{q_{1,\nu}q_{2,\mu}}{4q_{12}} + \frac{q_{1,\nu}q_{3,\mu}q_{23}}{2q_{12}q_T^2} + \frac{q_{2,\mu}q_{3,\nu}q_{13}}{2q_{12}q_T^2} - \frac{q_{3,\mu}q_{3,\nu}}{2q_T^2}$$

$$\begin{aligned}
& + \frac{1}{(2-4\epsilon)} \left[\frac{q_{1,\nu} q_{2,\mu} q_{33}}{2q_{12} q_T^2} - \frac{q_{1,\nu} q_{2,\mu}}{2q_{12}} - \frac{q_{1,\nu} q_{3,\mu} q_{23}}{q_{12} q_T^2} - \frac{q_{2,\mu} q_{3,\nu} q_{13}}{q_{12} q_T^2} + \frac{q_{3,\mu} q_{3,\nu}}{q_T^2} + g_{\mu\nu} \right], \\
P_{2,\mu\nu} = & \frac{q_{1,\nu} q_{2,\mu} q_{33}}{4q_{12} q_T^2} + \frac{q_{1,\nu} q_{2,\mu}}{4q_{12}} - \frac{q_{1,\nu} q_{3,\mu} q_{23}}{2q_{12} q_T^2} - \frac{q_{2,\mu} q_{3,\nu} q_{13}}{2q_{12} q_T^2} + \frac{q_{3,\mu} q_{3,\nu}}{2q_T^2} \\
& + \frac{1}{(2-4\epsilon)} \left[\frac{q_{1,\nu} q_{2,\mu} q_{33}}{2q_{12} q_T^2} - \frac{q_{1,\nu} q_{2,\mu}}{2q_{12}} - \frac{q_{1,\nu} q_{3,\mu} q_{23}}{q_{12} q_T^2} - \frac{q_{2,\mu} q_{3,\nu} q_{13}}{q_{12} q_T^2} + \frac{q_{3,\mu} q_{3,\nu}}{q_T^2} + g_{\mu\nu} \right].
\end{aligned} \tag{8}$$

The partonic cross section is obtained from $|\mathcal{M}|^2$ after integration over the phase space and multiplication by the flux factor.

3 One-loop considerations

Before providing details on our two-loop calculation we want to investigate the quality of the high-energy expansion at one-loop order. In the following we consider the differential partonic cross section

$$\frac{d\sigma}{d\theta}(s, t) \tag{9}$$

where the scattering angle θ of the Higgs boson in the center-of-mass frame enters via the following relation,

$$t = -\frac{s}{2}(1 - \cos\theta). \tag{10}$$

In Fig. 1 we study the \sqrt{s} -dependence of $d\sigma/d\theta$ for fixed scattering angle θ of 90 degrees. The exact result (see the solid curve for $m_H \neq 0$ and the short-dashed curve for $m_H = 0$) is compared to various approximation, computed for $m_H = 0$, incorporating high-energy expansions up to m_t^{32} (see the long-dashed and dash-dotted curves). For comparison we also show the result based on an effective-theory calculation in which the limit of infinite top quark mass is assumed (dotted curve). We observe that, as expected, the high-energy approximations lead to good results for large values of \sqrt{s} . A systematic improvement is obtained after including higher order expansion terms. For example, for $\sqrt{s} \approx 1500$ GeV the curves including m_t^8 and m_t^{16} terms agree with each other and the exact (short-dashed) curve which suggests that an approximation incorporating m_t^8 terms works well above this energy. With the same argument we conclude that m_t^{16} terms are sufficient to describe the exact result down to $\sqrt{s} \approx 750$ GeV. It seems that one cannot go significantly below this energy since both the m_t^{16} and the m_t^{32} curves start to diverge just below $\sqrt{s} \approx 750$ GeV.

In the evaluation of the master integrals we assume $m_t^2 \ll s, t$. This means that the expansion breaks down for $\theta \rightarrow 0, \pi$ (where $|t|$ becomes small) and thus a restricted phase

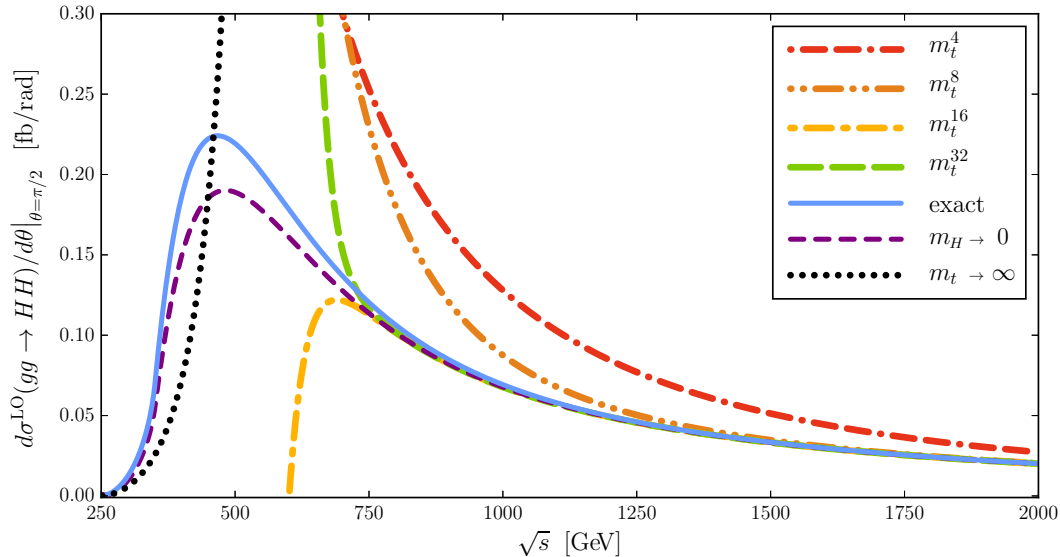


Figure 1: $d\sigma/d\theta$ as a function of \sqrt{s} for fixed $\theta = \pi/2$.

space has to be considered when performing the integration over θ . In practical applications this does not constitute a big problem since $\theta \rightarrow 0, \pi$ corresponds to the forward and backward scattering of the Higgs boson, where no measurement can be performed. Furthermore, the bulk of the cross section is provided by the central region. For example, if we restrict $0.25\pi < \theta < 0.75\pi$ in the exact one-loop corrections we cover around 70% of the full cross section for $\sqrt{s} = 1000$ GeV.

Apart from providing an independent and analytically simple expression in the high energy region, which can be used as a cross-check of the exact (numerical) results, our expressions also serve as input of the method based on Padé approximants [22] as already mentioned in the Introduction.

4 Reduction to master integrals

We generate our amplitudes with the program `qgraf` [24] and use `q2e` and `exp` [25, 26] to rewrite the output to `FORM` [27] notation. `exp` is also used to assign to each Feynman diagram an integral family which is defined according to the topology and mass distribution of the internal lines. For our application we have defined 34 families. We use `FORM` to express the amplitude for each diagram as a linear combination of scalar integrals of a given family.

We use the `C++` version of `FIRE` [28] for the reduction of all scalar integrals from each family to master integrals, with `LiteRed` [29, 30] providing `#rules` for `FIRE`. All families were reduced using the publicly available version `FIRE 5.2`. Some families were also re-

duced using the development versions FIRE 5.5, 5.6 (which use more information from the `LiteRed` files) in order to check whether the number of master integrals produced was smaller. This was the case, but the number of master integrals was still not minimal. We describe our procedure to obtain a minimal set of master integrals below. The `Mathematica`-readable tables generated by FIRE are transformed to `FORM Fill` statements, so that the reduction can be applied to the amplitude in `FORM` using a `TableBase`. The reduction rules are heavily manipulated in `FORM` before creating this `TableBase`.

After the FIRE reduction, each integral family contains between 7 and 77 master integrals (1395 in total (1+2 loops)). One must minimize the number of master integrals between all families; the use of FIRE’s `FindRules[]` command yields a total of $231 = 10 + 221$ master integrals. This does not constitute a minimal set. We use the following procedure, implemented in `FORM`, to find and eliminate “master integrals” which are in fact a linear combination of other integrals of the set.

1. For each n -line master integral with a dot on one of its lines, generate the $n - 1$ integrals which instead have a dot on one of the other lines. Append these integrals to the set of integrals from the amplitude. Ensure that each integral in this extended set is present in the reduction tables.
2. Apply relations from `FindRules[]` to the extended set of integrals and consider equations of the form:

$$\text{FindRules}[I] == I. \tag{11}$$

Apply the reduction tables to these equations and discard all trivial equations. One obtains a set of non-trivial equations which relate some integrals in the original set of master integrals.

3. Use these equations to construct reduction relations into a final linearly independent set of master integrals. We solve the equations to obtain the “most complicated” (highest line count) integrals in terms of simpler integrals.

In Step 2, we consider such equations for all integrals I of complexity < 9 , where we define the complexity as the sum of the absolute values of the propagator powers. The reduction rules for higher complexity integrals contain coefficients which are too large to efficiently manipulate with `FORM`’s `PolyRatFun`. Despite this, the set of equations contains many redundancies. That these equations are all satisfied increases our confidence that our final set of master integrals is a minimal set. Additionally, `FindRules[]` maps many integrals into different integral families, so this procedure shows some consistency between our families. We note that no approximation (except $m_H = 0$) is applied during the reduction procedure. In particular, we retain the exact m_t dependence.

Following this procedure we reduce the number of two-loop master integrals from 221 to 161. A list of them, and all 10 one-loop¹ master integrals, can be found in Appendix A.

¹Note that only 7 of these 10 master integrals appear in the amplitude.

At one-loop order we obtain the minimal set of ten master integrals simply by applying `FindRules[]` to the master integrals of the three one-loop families. The additional two-loop reduction relations are applied to the `FIRE` reduction relations before we create the `FORM TableBase` which we apply to the amplitude and to the right-hand-side of differential equations (see Subsection 5.1).

The computation of these master integrals is described in Section 5.

5 Calculation of master integrals

For the calculation of the master integrals we use the method of differential equations [31, 32]. We solve the differential equations using an appropriate ansatz which is described in Subsection 5.1. The boundary conditions (see Subsection 5.2) are fixed by evaluating the master integrals in the limit $m_t \rightarrow 0$. In some cases it is sufficient to evaluate the integrals in this limit for fixed $t = s = -1$.

5.1 Differential equations

We compute the master integrals in an unphysical region where two Mandelstam variables (s and t) are negative and u is positive. In this region, the integrals which we compute are real valued. We can analytically continue results obtained here into the physical region.

For each master integral we have three differential equations which are obtained by taking derivatives w.r.t. m_t^2 , s and t . The derivatives are computed using `LiteRed`. Note that only two of the three differential equations are needed to construct the result. The third provides a consistency check. The generation of the system of differential equations requires the extension of the `FIRE` reduction tables. Note, however, that the additional integrals which are required are not difficult to reduce.

Differentiating the vector of master integrals, (MI) , w.r.t. $x = t, m_t^2$ and applying the reduction tables to the result leads to systems of equations

$$\frac{d}{dx}(MI) = K_x \cdot (MI), \quad (12)$$

where K_x is a square matrix.

To solve the differential equations we follow two approaches. In the first, we make an ansatz for each master integral which is suitable to describe the solution in the limit $m_t \rightarrow 0$. Guided by asymptotic expansion we use (see also Refs. [18, 33])

$$I = \sum_{n_1=n_1^{\min}}^{\infty} \sum_{n_2=n_2^{\min}}^{\infty} \sum_{n_3=0}^{2l+n_1} c(I, n_1, n_2, n_3, s, t) \epsilon^{n_1} (m_t^2)^{n_2} (\log(m_t^2))^{n_3}, \quad (13)$$

where l is the number of loops. To determine the coefficients c of the ansatz we use the following procedure:

- (1) Use the differential equation for t and determine the coefficients of the leading terms in the $m_t \rightarrow 0$ expansion. This requires the solution of a system of first-order differential equations for the t -dependent coefficients c . Boundary conditions are needed for one specific value of t , e.g., for $t = s = -1$.
- (2) Use the differential equation for m_t^2 to obtain relations between the coefficients of the higher order m_t^2 terms and the leading terms determined in (1). Since the m_t dependence is explicit in the ansatz one only has to solve a system of linear equations.
- (3) The results for the master integrals are inserted into the differential equation for s , which must be satisfied.

At one-loop order the matrix K_t in Eq. (12) has a triangular structure. Thus, starting from the simplest integral, one can run through the vector of master integrals and solve the system integral-by-integral.

At two-loop order K_t in Eq. (12) rather has a block-triangular structure. It contains blocks of up to four integrals, which form coupled systems of differential equations. The integrals within these blocks must be determined together.

Using the above approach based on t -independent boundary conditions we were not able to obtain results for all two-loop master integrals. Presumably this is due to an inconvenient choice of our set of master integrals. For this reason we developed a second approach where we determine the master integrals in the limit $m_t^2 \rightarrow 0$, keeping the full t dependence. Afterwards we only have to solve the m_t^2 differential equation which, as mentioned above, reduces to solving a system of linear equations. This approach provides results for all master integrals. Where possible, we compared the results of the two approaches and found complete agreement.

Let us end this subsection by making a brief comment on the possibility to introduce a canonical basis [34] for our master integrals. We made several attempts to produce such a basis using the publicly available programs `Fuchsia` [35] and `CANONICA` [36]. We were not able to obtain a canonical basis for our master integrals for all sectors. Since we are interested in the small- m_t limit we did not insist on obtaining a canonical basis.

5.2 Boundary conditions

The main tools which we use to compute the boundary conditions are the method of regions [37, 38] and Mellin-Barnes techniques (see, e.g., [38]). Additionally, we make use of the PSLQ algorithm [39] and exploit the anticipated dependence on irrational numbers of our final result to obtain exact expressions.

In the following we provide details of each step of the calculation and give concrete examples for the master integral $G_6(1, 1, 1, 1, 1, 1, 1, 0, 0)$. See Appendix A for definitions of the integral families.

In this section we assume the scaling

$$m_t^2 \sim \chi, \quad s \sim 1, \quad t \sim 1, \quad (14)$$

where the parameter $\chi \ll 1$ is introduced for convenience.

To begin, we express the Feynman integral in its alpha representation (using the routines provided in FIESTA [40]). This is a convenient starting point to apply the method of regions. For example, the integral $G_6(1, 1, 1, 1, 1, 1, 1, 0, 0)$ is expressed as

$$J = (\mu^2)^{2\epsilon} e^{2\epsilon\gamma_E} \left(\prod_{i=1}^7 \int_0^\infty \alpha_i^{\delta_i} \right) \mathcal{U}^{-d/2} \exp(-\mathcal{F}/\mathcal{U}), \quad (15)$$

where the functions \mathcal{U} and \mathcal{F} , the so-called first and second Symanzik polynomials, are given by

$$\begin{aligned} \mathcal{U} &= \alpha_1\alpha_4 + \alpha_1\alpha_5 + \alpha_1\alpha_6 + \alpha_1\alpha_7 + \alpha_2\alpha_4 + \alpha_2\alpha_5 + \alpha_2\alpha_6 + \alpha_2\alpha_7 \\ &\quad + \alpha_3\alpha_4 + \alpha_3\alpha_5 + \alpha_3\alpha_6 + \alpha_3\alpha_7 + \alpha_4\alpha_7 + \alpha_5\alpha_7 + \alpha_6\alpha_7, \\ \mathcal{F} &= m_t^2 (\alpha_1 + \alpha_2 + \alpha_3 + \alpha_4 + \alpha_5 + \alpha_6) \mathcal{U} - t (\alpha_2\alpha_5\alpha_7) - s (\alpha_1\alpha_3\alpha_4 + \alpha_1\alpha_3\alpha_5 \\ &\quad + \alpha_1\alpha_3\alpha_6 + \alpha_1\alpha_3\alpha_7 + \alpha_1\alpha_4\alpha_6 + \alpha_1\alpha_4\alpha_7 + \alpha_2\alpha_4\alpha_6 + \alpha_3\alpha_4\alpha_6 + \alpha_3\alpha_6\alpha_7 + \alpha_4\alpha_6\alpha_7). \end{aligned} \quad (16)$$

In Eq. (15) we have introduced analytic regularization parameters δ_i to regularize collinear divergences, which appear later in the calculation. The original integral is obtained by taking the sequence limit $\delta_i \rightarrow 0$ for all δ_i .

To implement the asymptotic expansion for $\chi \rightarrow 0$ we use the program `asy.m` [41]. It provides scaling rules for the alpha parameters for the various regions which have to be considered. For the integral in Eq. (15) there are 13 relevant regions. One corresponds to the so-called hard region, in which all seven alpha parameters scale as “1”. There are twelve so-called soft-collinear regions where some of the parameters have the weight “1” and others the weight “ χ ”. For example, for region 2, we have that

$$\text{region 2 : } \quad \{\alpha_1 \sim \chi, \alpha_2 \sim 1, \alpha_3 \sim 1, \alpha_4 \sim 1, \alpha_5 \sim \chi, \alpha_6 \sim \chi, \alpha_7 \sim 1\}. \quad (17)$$

In total only four regions need to be considered. The remaining eight regions can be obtained by simple symmetry considerations.

After the expansion, the original integral is expressed as a sum of homogeneously scaling integrals

$$J = (\mu^2)^{2\epsilon} e^{2\epsilon\gamma_E} \sum_{n=1}^{13} \left(\prod_{i=1}^7 \int_0^\infty \alpha_i^{\delta_i} \right) \mathcal{U}_{(n)}^{-d/2} \exp(-\mathcal{F}_{(n)}/\mathcal{U}_{(n)}) + \mathcal{O}(\chi), \quad (18)$$

where the summation n spans the relevant regions and the subscript “ (n) ” indicates that the polynomials \mathcal{U} and \mathcal{F} from Eq. (16) are specific to the corresponding region. They are expanded to leading order in χ . Note that each integral on the r.h.s. is homogeneous in m_t^2 (or χ) but not in s and t , since they are $\mathcal{O}(1)$ parameters.

In the hard region there is only one soft parameter, m_t^2 , and thus a naive Taylor expansion of the integrand has to be performed. This leads to purely massless integrals which are known in the literature [42, 43]. We have cross-checked these results up to the order in ϵ necessary for our application. Note that the contribution of the hard region is regular in δ_i which means that one can take the limit $\delta_i \rightarrow 0$ at the very beginning.

The soft-collinear regions are more involved. In the following we outline the calculation of the contribution from region 2 as an example. The calculation for other regions proceeds analogously.

1. We express each integral in terms of two-dimensional Mellin-Barnes integrals. For our example integral, we find the following form

$$\begin{aligned}
J^{(2)} &= (\mu^2)^{2\epsilon} e^{2\epsilon\gamma_E} \int \frac{dz_1}{2\pi i} \frac{dz_2}{2\pi i} \frac{(-s)^{-\delta_{16}-2} (-t)^{-\delta_5-1} (m_t^2)^{-2\epsilon-\delta_{2347}} \Gamma(\epsilon + \delta_{47})}{\Gamma(\delta_2 + 1)\Gamma(\delta_3 + 1)\Gamma(\delta_4 + 1)\Gamma(\delta_7 + 1)\Gamma(-\epsilon - \delta_{156} - 1)} \\
&\quad \times \frac{\Gamma(-z_1)\Gamma(-z_2)\Gamma(z_2 - \epsilon - \delta_7 + 1)\Gamma(z_1 - \delta_5 + \delta_7)\Gamma(z_1 - \epsilon - \delta_{156} - 1)}{\Gamma(-\epsilon - \delta_{15} + z_1)\Gamma(-\epsilon - \delta_5 + z_{12} + 1)\Gamma(2\epsilon + \delta_{34} + 2\delta_7 - z_2)} \\
&\quad \times \Gamma(\epsilon + \delta_{37} - z_2)\Gamma(\delta_2 - \delta_5 + z_{12})\Gamma(z_{12} - \epsilon - \delta_{15})\Gamma(2\epsilon + \delta_{3457} - z_{12}), \tag{19}
\end{aligned}$$

where $z_{12} = z_1 + z_2$, $\delta_{123} = \delta_1 + \delta_2 + \delta_3$ and so on. Note that the integration contours of z_1 and z_2 are chosen to be straight lines parallel to the imaginary axis, satisfying $-1 < \text{Re}(z_1) < \text{Re}(z_2) < 0$.

2. Next we use the package `MB.m` [44] to analytically continue the regularization parameters δ_i and ϵ to zero. As a result we obtain two-dimensional Mellin-Barnes representations which depend only on z_1, z_2 and possibly on t/s . Note that the poles in δ_i cancel among the contributions from the different regions, which provides a good check of our calculations.
3. We now transform the two-dimensional Mellin-Barnes integrals into one-dimensional integrals. In general this step is non-trivial; we provide more details in Appendix B. For simple cases `barnesroutines.m` [45] can be used.
4. At this point we arrive at two types of one-dimensional integral: those which are independent of t/s and others which depend on t/s , such as

$$\int \frac{dz_1}{2\pi i} \left(\frac{t}{s}\right)^{z_1} \Gamma(-1 - z_1)^2 \Gamma(-z_1) \Gamma(1 + z_1)^2 \Gamma(2 + z_1) \psi(1 + z_1) \psi'(-z_1). \tag{20}$$

We perform a high-precision numerical evaluation (300 digits) of the t -independent integrals and, after summing the contributions from all regions, apply the PSLQ algorithm [39] to re-construct the analytic result as a rational linear combination of 33 products (up to weight 6) of numbers from the set

$$\{1, \ln 2, \pi^2, \zeta_3, \pi^4, \text{Li}_4(1/2), \zeta_5, \text{Li}_5(1/2), \pi^6, \text{Li}_6(1/2), S_{3,3}(-1)\}, \quad (21)$$

and use a further 200 digits to verify each result. The Nielsen generalized polylogarithm $S_{3,3}(-1)$ is implemented in **Mathematica** as `PolyLog[3,3,-1]`.

For the t -dependent integrals we make an ansatz containing harmonic polylogarithms (HPLs) [46] up to weight 6 with alphabet $\nu_i \in \{-1, 0\}$,

$$\sum_{n=0}^6 c_{\{\nu_i\},n} \text{H}(\{\nu_i\}, t/s) \log^n(-m_t^2/s), \quad (22)$$

which we Taylor-expand in t/s . The series is expressed as a multivariate polynomial in $(t/s), \log(t/s), \log(-m_t^2/s)$. We obtain the Taylor series of the integrals by taking their residues at $z_1 = 0, 1, 2, 3, \dots$. We then use 50 low-order terms of the Taylor series to fix the coefficients $c_{\{\nu_i\},n}$ of the ansatz and check the result using a further 200 higher-order terms of the Taylor series.

Using the above procedure, we obtain the following δ_i -independent result for our sample master integral $G_6(1, 1, 1, 1, 1, 1, 1, 0, 0)$,

$$\begin{aligned} J = & -\left(\frac{\mu^2}{-s}\right)^{2\epsilon} \frac{1}{s^2 t} \left\{ l_m^4 - \frac{8}{3} l_m^3 l_t + l_m^2 \left(2l_t^2 - \frac{2\pi^2}{3} \right) + l_m \left(\frac{8\pi^2}{3} l_t - 4\zeta_3 \right) \right. \\ & - \frac{7\pi^4}{15} + 4l_t \zeta_3 - 2\pi^2 l_t^2 - \frac{1}{3} l_t^4 + 8H(-2, 0, 0; t/s) + 4\pi^2 H(-2; t/s) \\ & + \epsilon \left[-\frac{4}{3} l_m^5 + \frac{19}{6} l_m^4 l_t + l_m^3 \left(-\frac{4\pi^2}{9} - 2l_t^2 \right) \right. \\ & + l_m^2 \left(-4\zeta_3 + \pi^2 l_t + \frac{1}{3} l_t^3 - \pi^2 H(-1, t/s) - 2H(-1, 0, 0; t/s) \right) \\ & + l_m \left(-\frac{11\pi^4}{45} + 8\zeta_3 l_t - \frac{10\pi^2}{3} l_t^2 - \frac{2}{3} l_t^4 + 8H(-2, 0, 0; t/s) + 8H(-1, 0, 0, 0; t/s) \right. \\ & + 4\pi^2 H(-2; t/s) + \left. \left. \frac{4\pi^2}{3} H(-1, 0; t/s) \right) - 52\zeta_5 + 6\pi^2 \zeta_3 + \frac{83\pi^4}{90} l_t - 4\zeta_3 l_t^2 + \frac{25\pi^2}{9} l_t^3 + \frac{l_t^5}{2} \right. \\ & - 22\pi^2 H(-3; t/s) - \frac{23\pi^4}{30} H(-1; t/s) + 16\pi^2 H(-2, 1; t/s) + 6\pi^2 H(-1, -2; t/s) \\ & - 44H(-3, 0, 0; t/s) - \frac{10\pi^2}{3} H(-1, 0, 0; t/s) + 32H(-2, -1, 0, 0; t/s) \\ & \left. - 48H(-2, 0, 0, 0; t/s) + 12H(-1, -2, 0, 0; t/s) - 12H(-1, 0, 0, 0, 0; t/s) \right\} \end{aligned}$$

$$\left. \left. \left. +32\zeta_3 H(-2; t/s) - 24\zeta_3 H(-1, 0; t/s) - \frac{40\pi^2}{3} H(-2, 0; t/s) \right] \right\} + \mathcal{O}(m_t^2) + \mathcal{O}(\epsilon^2), \quad (23)$$

where $l_m = \log(-m_t^2/s)$ and $l_t = \log(t/s)$.

To solve the m_t^2 -differential equation for most of our master integrals, it is sufficient to obtain just the leading term in the small- m_t expansion of the boundary condition. However, for 9 integrals it is also necessary to compute the next-to-leading term in the asymptotic expansion. In most of these cases we can simply apply the method discussed above and expand up to the next-to-leading term in χ . However, for two of the seven-line integrals, Step 3 above is hard to apply at the next-to-leading order. For these integrals, we use the corresponding t -differential equations to obtain the next-to-leading boundary conditions.

For example, the next-to-leading term of $G_6(1, 1, 1, 1, 1, 1, 2, 0, 0)$ is determined in the following way: we consider the t -differential equation of $G_6(1, 1, 1, 1, 1, 1, 1, 0, 0)$, which is fully known at the leading order,

$$\begin{aligned} \frac{d}{dt} G_6(1, 1, 1, 1, 1, 1, 1, 0, 0) &= +A G_6(1, 1, 1, 1, 1, 1, 1, 0, 0) \\ &+ B m_t^2 G_6(1, 1, 1, 1, 1, 2, 1, 0, 0) \\ &+ C G_6(1, 1, 1, 1, 1, 1, 2, 0, 0) \\ &+ (\text{known lower-line integrals}) \end{aligned} \quad (24)$$

where A , B and C are $\mathcal{O}(1)$ coefficients. The leading terms of the integrals behave as follows,

$$\begin{aligned} G_6(1, 1, 1, 1, 1, 1, 1, 0, 0) &= \mathcal{O}(1) \\ G_6(1, 1, 1, 1, 1, 2, 1, 0, 0) &= \mathcal{O}(1/m_t^2) \\ G_6(1, 1, 1, 1, 1, 1, 2, 0, 0) &= \mathcal{O}(1/m_t^2). \end{aligned} \quad (25)$$

Therefore, the next-to-leading ($\mathcal{O}(1)$) contribution to $G_6(1, 1, 1, 1, 1, 1, 2, 0, 0)$ appears in the differential equation at $\mathcal{O}(1)$ alongside the (known) leading contributions to $G_6(1, 1, 1, 1, 1, 1, 1, 0, 0)$ and $G_6(1, 1, 1, 1, 1, 2, 1, 0, 0)$ and can be easily determined. Note that the leading order ($\mathcal{O}(1/m_t^2)$) contribution of $G_6(1, 1, 1, 1, 1, 1, 2, 0, 0)$ cancels against $\mathcal{O}(1/m_t^2)$ terms from the lower-line integrals appearing in Eq. (24).

We have checked all boundary conditions numerically at a few euclidian values of s and t using the command `SDExpandAsy` of `FIESTA` [40].

5.3 Solving the differential equations

Using the boundary conditions discussed in the previous subsection we can solve the differential equations of Subsection 5.1 in a straightforward way. All of our results are expressed in terms of HPLs. The expansion depth is limited only by the size of the

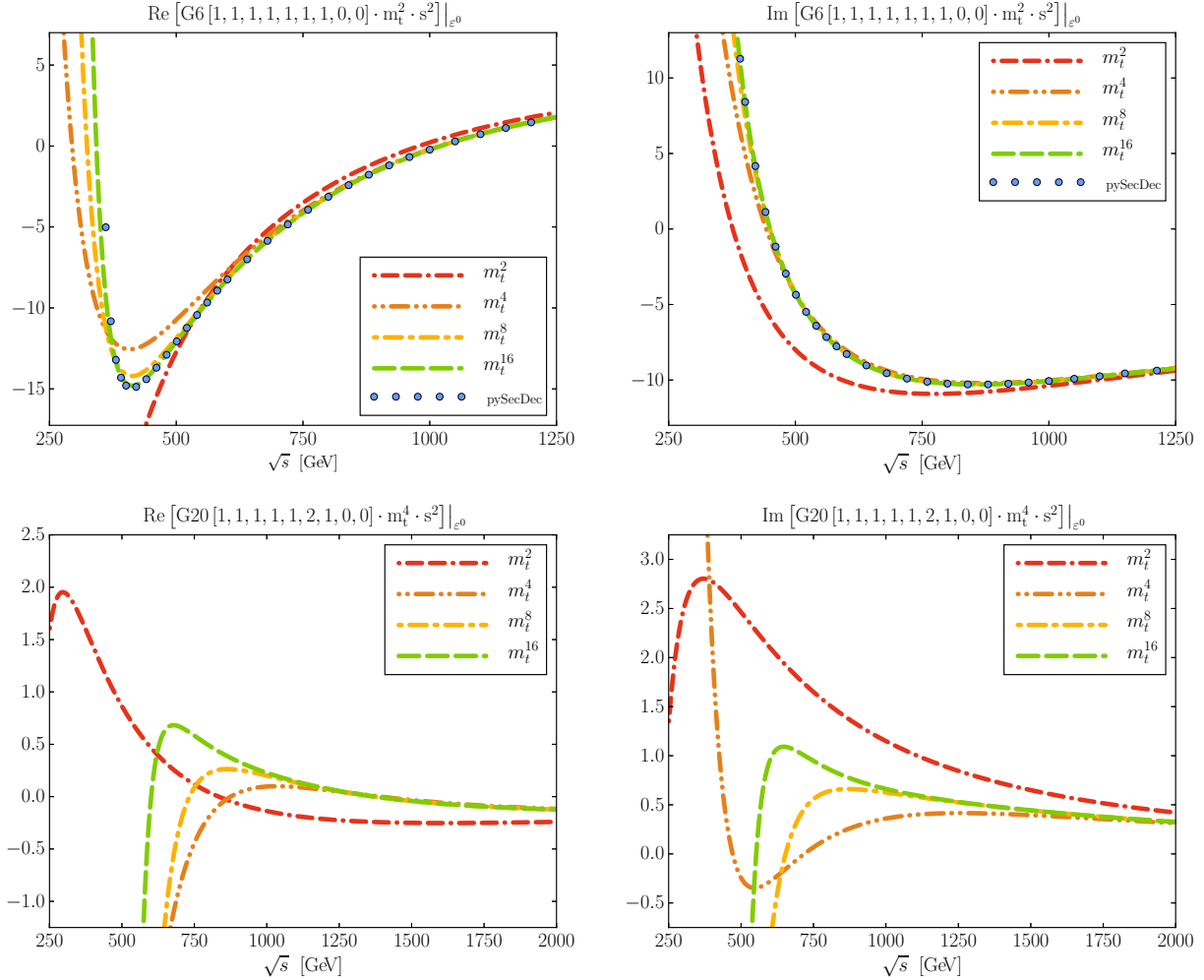


Figure 2: Real and imaginary part of the ϵ^0 term of the two master integrals $G_6(1, 1, 1, 1, 1, 1, 1, 0, 0)$ and $G_{20}(1, 1, 1, 1, 1, 2, 1, 0, 0)$. For convenience we multiply by powers of m_t and s as indicated above the plot.

intermediate expressions which enter the system of linear equations for the coefficients in our ansatz. We have expanded each master integral such that the final result for the amplitude $gg \rightarrow HH$ is available up to order m_t^{16} . Our results for the master integrals can be downloaded from [23].

For illustration we show in Fig. 2 the results for two master integrals: $G_6(1, 1, 1, 1, 1, 1, 1, 0, 0)$, which is used as an example in Subsection 5.2, and $G_{20}(1, 1, 1, 1, 1, 2, 1, 0, 0)$. We plot the real and imaginary parts of the ϵ^0 term as a function of \sqrt{s} and choose $t = -s/2$, which corresponds to $\theta = \pi/2$ (cf. Fig. 1), $m_t = 175$ GeV and $\mu^2 = s$. For clarity we multiply each integral by appropriate powers of m_t and s such that the leading term starts with m_t^2 and is dimensionless. In each case we display the approximations including m_t^2 , m_t^4 , m_t^8 and m_t^{16} terms.

In the panels showing $G_6(1, 1, 1, 1, 1, 1, 1, 0, 0)$ we compare the approximations to the exact result, which has been obtained numerically using `pySecDec` [47]. For this integral we observe a rapid convergence. In fact, the m_t^4 , m_t^8 and m_t^{16} curves agree with each other and the exact points down to $\sqrt{s} \approx 600$ GeV and the two highest approximation even down to $\sqrt{s} \approx 500$ GeV. It is interesting to note that the m_t^{16} curve reproduces to high accuracy the turning point at $\sqrt{s} \approx 400$ GeV and the steep rise below that energy. It can not be expected that all master integrals show such good convergence properties. In fact there are integrals, in particular some of the non-planar contributions, where the expansion parameter is m_t^2/u instead of m_t^2/s which results in a smaller radius of convergence.

For $G_{20}(1, 1, 1, 1, 1, 2, 1, 0, 0)$ we were not able to obtain stable numerical results using `pySecDec` and thus we only show our approximations. We observe a similar pattern as for the LO cross section shown in Fig. 1: the inclusion of more terms extends the convergence range in \sqrt{s} down to smaller values. Furthermore, the curves including m_t^8 and m_t^{16} terms agree down to $\sqrt{s} \approx 900$ GeV and it can be expected that above this energy a good approximation to the exact result can be provided.

6 Conclusions

The main focus of this paper is on NLO corrections to double Higgs boson production in the high energy region, where the top quark mass is assumed to be small compared to the kinematic variables s and t . Such considerations complement expansions for large top quark mass and around the threshold which have been considered in the literature, see Refs. [4, 22]. Furthermore, they provide an independent cross check of the exact calculation [15] which relies heavily on numerical methods.

In this paper we perform the reduction of the $gg \rightarrow HH$ amplitude to master integrals and compute all planar integrals in an expansion for small m_t^2 . The expansion depth for each master integral is chosen such that the amplitude includes terms up to order m_t^{16} . Our analytic results for the master integrals are expressed in terms of HPLs and can be obtained in computer-readable form from [23].

Acknowledgements

This work is supported by the BMBF grant 05H15VKCCA. D.W. acknowledges the support by the DFG-funded Doctoral School KSETA. We thank Alexander Smirnov for providing us with unpublished versions of `FIRE` which we could use to help optimize our reduction. We thank Alexander Smirnov and Vladimir Smirnov for many useful discussions.

A One- and two-loop master integrals

We define the propagators of the one-loop integral family as

$$D_1(q_1, q_2, q_3, q_4) = \{m_t^2 - l_1^2, m_t^2 - (l_1 + q_3)^2, m_t^2 - (l_1 - q_1 - q_2)^2, m_t^2 - (l_1 - q_1)^2\}, \quad (26)$$

and at two loops we introduce

$$\begin{aligned} D_6(q_1, q_2, q_3, q_4) &= \{m_t^2 - l_1^2, m_t^2 - l_2^2, m_t^2 - (l_2 + q_3)^2, m_t^2 - (l_2 - q_1 - q_2)^2, \\ &\quad m_t^2 - (l_1 - q_1 - q_2)^2, m_t^2 - (l_1 - q_1)^2, -(l_1 - l_2)^2, -(l_1 + q_3)^2, \\ &\quad -(l_2 + q_1)^2\}, \\ D_{20}(q_1, q_2, q_3, q_4) &= \{-l_1^2, m_t^2 - l_2^2, m_t^2 - (l_2 + q_3)^2, m_t^2 - (l_2 - q_1 - q_2)^2, \\ &\quad -(l_1 - q_1 - q_2)^2, -(l_1 - q_1)^2, m_t^2 - (l_1 - l_2)^2, -(l_1 + q_3)^2, -(l_2 + q_1)^2\}, \\ D_{33}(q_1, q_2, q_3, q_4) &= \{-l_1^2, m_t^2 - l_2^2, m_t^2 - (l_2 + q_4)^2, -(l_1 + q_3 + q_4)^2, -(l_1 - q_1)^2, \\ &\quad m_t^2 - (l_1 - l_2 + q_3)^2, m_t^2 - (l_1 - l_2)^2, -(l_1 + q_4)^2, -(l_2 + q_1)^2\}, \\ D_{47}(q_1, q_2, q_3, q_4) &= \{-l_1^2, m_t^2 - l_2^2, m_t^2 - (l_2 + q_4)^2, m_t^2 - (l_2 - q_1 - q_2)^2, \\ &\quad m_t^2 - (l_1 - l_2 + q_2)^2, m_t^2 - (l_1 - l_2)^2, -(l_1 - q_1)^2, -(l_1 + q_4)^2, \\ &\quad -(l_2 + q_1)^2\}, \\ D_{72}(q_1, q_2, q_3, q_4) &= \{m_t^2 - l_1^2, m_t^2 - (l_1 + q_2)^2, m_t^2 - (l_1 + q_1 + q_2)^2, m_t^2 - (l_2 + q_1 + q_2)^2, \\ &\quad m_t^2 - (l_2 - q_3)^2, m_t^2 - (l_1 - q_3)^2, -(l_1 - l_2)^2, -(l_2 + q_2)^2, -(l_2 + q_3)^2\}, \\ D_{75}(q_1, q_2, q_3, q_4) &= \{m_t^2 - l_1^2, m_t^2 - (l_1 + q_4)^2, m_t^2 - (l_1 - q_1 - q_2)^2, -(l_2 - q_1 - q_2)^2, \\ &\quad -(l_2 - q_1)^2, m_t^2 - (l_1 - q_1)^2, m_t^2 - (l_1 - l_2)^2, -(l_2 + q_4)^2, -(l_2 + q_1)^2\}, \\ D_{90}(q_1, q_2, q_3, q_4) &= \{m_t^2 - l_1^2, m_t^2 - (l_1 + q_3)^2, -(l_1 + l_2 - q_1 - q_2)^2, -(l_1 + l_2 - q_1)^2, \\ &\quad m_t^2 - (l_1 - q_1)^2, m_t^2 - (l_2 + q_4)^2, m_t^2 - l_2^2, -(l_2 + q_3)^2, -(l_2 + q_1)^2\}, \end{aligned}$$

where l_1 and l_2 are the loop momenta. Note that we prefer to use our internal notation for the families, which is the reason why the numbering is not sequential. We also define the integral families which are obtained by the exchange of external momenta. At one-loop order there are two more families which are related to $D_1(q_1, q_2, q_4, q_3)$ as follows,

$$D_2(q_1, q_2, q_3, q_4) = D_1(q_1, q_2, q_4, q_3) \quad D_3(q_1, q_2, q_3, q_4) = D_1(q_1, q_4, q_3, q_2). \quad (27)$$

At two-loop order we have

$$\begin{aligned} D_4(q_1, q_2, q_3, q_4) &= D_6(q_1, q_4, q_3, q_2) & D_5(q_1, q_2, q_3, q_4) &= D_6(q_1, q_2, q_4, q_3) \\ D_8(q_1, q_2, q_3, q_4) &= D_6(q_4, q_1, q_3, q_2) & D_{10}(q_1, q_2, q_3, q_4) &= D_6(q_3, q_1, q_4, q_2) \\ D_{11}(q_1, q_2, q_3, q_4) &= D_6(q_3, q_1, q_2, q_4) & D_{26}(q_1, q_2, q_3, q_4) &= D_{20}(q_4, q_3, q_1, q_2) \\ D_{51}(q_1, q_2, q_3, q_4) &= D_{47}(q_2, q_1, q_3, q_4) & D_{59}(q_1, q_2, q_3, q_4) &= D_{47}(q_2, q_3, q_1, q_4) \\ D_{71}(q_1, q_2, q_3, q_4) &= D_{72}(q_1, q_2, q_4, q_3) & D_{73}(q_1, q_2, q_3, q_4) &= D_{72}(q_1, q_4, q_2, q_3) \\ D_{78}(q_1, q_2, q_3, q_4) &= D_{75}(q_4, q_1, q_2, q_3) & D_{79}(q_1, q_2, q_3, q_4) &= D_{75}(q_2, q_1, q_3, q_4) \\ D_{84}(q_1, q_2, q_3, q_4) &= D_{75}(q_3, q_2, q_4, q_1) & D_{91}(q_1, q_2, q_3, q_4) &= D_{90}(q_4, q_1, q_2, q_3). \end{aligned} \quad (28)$$

Our minimal set of one-loop master integrals is given by

$$G_1(1, 1, 1, 1), \quad G_2(1, 0, 1, 0), \quad G_2(1, 1, 1, 0), \quad G_2(1, 1, 1, 1), \quad G_3(0, 0, 0, 1), \\ G_3(0, 1, 0, 1), \quad G_3(1, 0, 1, 0), \quad G_3(1, 1, 0, 1), \quad G_3(1, 1, 1, 0), \quad G_3(1, 1, 1, 1),$$

and at two loops we have

$$\begin{aligned}
& G_4(1, 1, 1, 1, 1, 1), \quad G_4(1, 1, 1, 1, 1, 2), \quad G_4(1, 1, 1, 1, 2, 1), \quad G_5(1, 1, 1, 1, 1, 1), \quad G_5(1, 1, 1, 1, 1, 2), \\
& G_5(1, 1, 1, 1, 2, 1), \quad G_6(1, 1, 0, 1, 1, 0, 0), \quad G_6(1, 1, 0, 1, 1, 1, 0), \quad G_6(1, 1, 1, 1, 1, 1, 0), \quad G_6(1, 1, 1, 1, 1, 1, 1), \\
& G_6(1, 1, 1, 1, 1, 2, 1), \quad G_6(1, 1, 1, 1, 1, 2, 1), \quad G_8(1, 1, 0, 1, 1, 0, 0), \quad G_8(1, 1, 0, 1, 1, 1, 0), \quad G_8(1, 1, 1, 1, 1, 1, 0), \\
& G_8(1, 1, 1, 1, 1, 1, 1), \quad G_8(1, 1, 1, 1, 1, 1, 2), \quad G_8(1, 1, 1, 1, 1, 2, 1), \quad G_8(1, 1, 1, 1, 1, 2, 1), \quad G_{10}(1, 1, 1, 1, 1, 1, 2), \\
& G_{10}(1, 1, 1, 1, 1, 2, 1), \quad G_{11}(1, 1, 0, 1, 1, 0, 0), \quad G_{11}(1, 1, 0, 1, 1, 1, 0), \quad G_{11}(1, 1, 1, 1, 1, 1, 0), \quad G_{11}(1, 1, 1, 1, 1, 1, 1), \\
& G_{11}(1, 1, 1, 1, 1, 2), \quad G_{11}(1, 1, 1, 1, 1, 2, 1), \quad G_{20}(1, 1, 0, 1, 1, 0, 0), \quad G_{20}(1, 1, 0, 1, 1, 0, 1), \quad G_{20}(1, 1, 1, 1, 1, 0, 0), \\
& G_{20}(1, 1, 1, 1, 1, 0, 1), \quad G_{20}(1, 1, 1, 1, 1, 1, 1), \quad G_{20}(1, 1, 1, 1, 1, 2), \quad G_{20}(1, 1, 1, 1, 1, 2, 1), \quad G_{20}(1, 1, 2, 1, 1, 1, 1), \\
& G_{26}(1, 1, 1, 1, 1, 1, 1), \quad G_{26}(1, 1, 1, 1, 1, 1, 2), \quad G_{26}(1, 1, 1, 1, 1, 2, 1), \quad G_{26}(1, 1, 2, 1, 1, 1, 1), \quad G_{33}(1, 0, 1, 1, 1, 0, 1), \\
& G_{33}(1, 0, 1, 1, 2, 0, 1), \quad G_{33}(1, 1, 0, 1, 0, 0, 0), \quad G_{33}(1, 1, 0, 1, 0, 1, 0), \quad G_{33}(1, 1, 0, 1, 0, 2, 0), \quad G_{33}(1, 1, 0, 1, 1, 1, 0), \\
& G_{33}(1, 1, 0, 1, 2, 1, 0), \quad G_{33}(1, 1, 1, 1, 0, 1, 0), \quad G_{33}(1, 1, 1, 1, 0, 1, 1), \quad G_{33}(1, 1, 1, 1, 0, 2, 1), \quad G_{33}(1, 1, 1, 1, 1, 0, 1), \\
& G_{33}(1, 1, 1, 1, 1, 1, 0), \quad G_{33}(1, 1, 1, 1, 1, 1, 1), \quad G_{33}(1, 1, 1, 1, 2, 1, 1), \quad G_{33}(1, 1, 1, 2, 1, 1, 1), \quad G_{33}(1, 1, 2, 1, 1, 1, 1), \\
& G_{47}(1, 0, 1, 1, 1, 2, 1), \quad G_{47}(1, 1, 1, 0, 1, 2, 1), \quad G_{47}(1, 1, 1, 1, 1, 1, 2), \quad G_{47}(1, 1, 1, 2, 1, 0, 0), \quad G_{47}(1, 1, 1, 2, 1, 1, 1), \\
& G_{51}(1, 1, 0, 1, 1, 1, 1), \quad G_{51}(1, 1, 1, 1, 1, 1, 1), \quad G_{51}(1, 1, 1, 1, 1, 2, 1), \quad G_{51}(1, 1, 1, 1, 2, 1, 1), \quad G_{51}(1, 0, 1, 1, 1, 1, 1), \\
& G_{59}(1, 1, 0, 1, 1, 1, 1), \quad G_{59}(1, 1, 1, 1, 1, 1, 1), \quad G_{59}(1, 1, 1, 1, 1, 2, 1), \quad G_{59}(1, 1, 1, 1, 2, 1, 1), \quad G_{59}(1, 2, 1, 1, 1, 1, 1), \\
& G_{59}(2, 1, 1, 1, 1, 1, 1), \quad G_{71}(1, 1, 1, 1, 1, 0, 1), \quad G_{71}(1, 1, 2, 1, 1, 0, 1), \quad G_{71}(1, 2, 0, 1, 0, 1, 1), \quad G_{72}(0, 1, 0, 1, 1, 2, 1), \\
& G_{72}(1, 0, 1, 1, 1, 0, 1), \quad G_{72}(1, 0, 2, 1, 1, 0, 1), \quad G_{72}(1, 1, 0, 1, 1, 0, 1), \quad G_{72}(1, 1, 0, 1, 1, 0, 2), \quad G_{72}(1, 1, 0, 1, 1, 0, 3), \\
& G_{72}(1, 1, 0, 1, 1, 1, 1), \quad G_{72}(1, 1, 0, 1, 1, 2, 1), \quad G_{72}(1, 1, 1, 1, 1, 0, 1), \quad G_{72}(1, 1, 2, 1, 1, 0, 1), \quad G_{73}(0, 1, 0, 1, 0, 1, 2), \\
& G_{73}(0, 1, 0, 1, 1, 2, 1), \quad G_{73}(0, 1, 1, 1, 1, 0, 1), \quad G_{73}(1, 0, 1, 1, 1, 0, 1), \quad G_{73}(1, 1, 0, 1, 1, 2, 1), \quad G_{73}(1, 1, 1, 1, 1, 0, 1), \\
& G_{73}(1, 1, 2, 1, 1, 0, 1), \quad G_{75}(1, 1, 0, 1, 0, 2, 1), \quad G_{78}(1, 1, 0, 1, 0, 1, 1), \quad G_{78}(1, 1, 0, 1, 0, 2, 1), \quad G_{78}(1, 1, 1, 0, 0, 1, 1), \\
& G_{78}(1, 1, 1, 0, 1, 0, 1), \quad G_{78}(1, 2, 1, 0, 1, 0, 1), \quad G_{78}(2, 1, 0, 1, 0, 1, 1), \quad G_{79}(1, 0, 1, 0, 0, 0, 1), \quad G_{79}(1, 0, 1, 0, 0, 1, 1), \\
& G_{79}(1, 0, 1, 0, 1, 0, 1), \quad G_{79}(1, 0, 1, 0, 1, 0, 2), \quad G_{79}(1, 0, 1, 0, 2, 0, 1), \quad G_{79}(1, 1, 1, 0, 0, 1, 1), \quad G_{79}(1, 1, 1, 0, 1, 0, 1), \\
& G_{79}(1, 2, 1, 0, 1, 0, 1), \quad G_{84}(0, 1, 0, 0, 2, 0, 1), \quad G_{84}(1, 0, 1, 0, 0, 0, 1), \quad G_{84}(1, 0, 1, 0, 0, 1, 1), \quad G_{84}(1, 0, 1, 0, 1, 0, 1), \\
& G_{84}(1, 0, 1, 0, 1, 0, 2), \quad G_{84}(1, 0, 1, 0, 2, 0, 1), \quad G_{84}(1, 1, 1, 0, 0, 1, 1), \quad G_{84}(1, 1, 1, 0, 1, 0, 1), \quad G_{84}(1, 2, 1, 0, 1, 0, 1), \\
& G_{84}(2, 1, 1, 0, 1, 0, 1), \quad G_{90}(1, 1, 1, 0, 1, 1, 1), \quad G_{90}(1, 1, 1, 1, 2, 1, 1), \quad G_{90}(1, 1, 1, 2, 1, 1, 1), \quad G_{90}(1, 2, 1, 0, 1, 1, 1), \\
& G_{91}(0, 0, 0, 0, 1, 0, 1), \quad G_{91}(0, 0, 1, 0, 1, 1, 0), \quad G_{91}(0, 0, 1, 0, 1, 1, 1), \quad G_{91}(0, 1, 0, 0, 1, 0, 1), \quad G_{91}(0, 1, 0, 1, 1, 0), \\
& G_{91}(0, 1, 0, 1, 1, 1), \quad G_{91}(0, 1, 0, 1, 1, 2, 0), \quad G_{91}(0, 1, 1, 1, 1, 1, 1), \quad G_{91}(1, 0, 0, 1, 0, 1, 0), \quad G_{91}(1, 0, 0, 1, 0, 1, 1), \\
& G_{91}(1, 0, 0, 1, 1, 1, 1), \quad G_{91}(1, 0, 0, 2, 0, 1, 0), \quad G_{91}(1, 0, 1, 0, 0, 0, 1), \quad G_{91}(1, 0, 1, 0, 0, 1, 1), \quad G_{91}(1, 0, 1, 0, 1, 1, 1), \\
& G_{91}(1, 0, 1, 1, 0, 1, 1), \quad G_{91}(1, 0, 1, 1, 1, 1, 0), \quad G_{91}(1, 0, 1, 1, 1, 1, 1), \quad G_{91}(1, 0, 1, 1, 1, 1, 2), \quad G_{91}(1, 0, 1, 1, 1, 2, 0), \\
& G_{91}(1, 0, 2, 0, 0, 0, 1), \quad G_{91}(1, 0, 2, 0, 1, 1, 1), \quad G_{91}(1, 0, 3, 0, 1, 1, 1), \quad G_{91}(1, 1, 0, 0, 1, 0, 1), \quad G_{91}(1, 1, 0, 1, 0, 1, 1), \\
& G_{91}(1, 1, 0, 1, 1, 1, 0), \quad G_{91}(1, 1, 0, 2, 0, 1, 1), \quad G_{91}(1, 1, 0, 3, 0, 1, 1), \quad G_{91}(1, 1, 1, 0, 0, 1, 1), \quad G_{91}(1, 1, 1, 0, 1, 0, 1), \\
& G_{91}(1, 1, 1, 0, 1, 1, 1), \quad G_{91}(1, 1, 1, 1, 0, 0, 1), \quad G_{91}(1, 1, 1, 1, 0, 0, 2), \quad G_{91}(1, 1, 1, 1, 0, 1, 1), \quad G_{91}(1, 1, 1, 1, 1, 1, 1), \\
& G_{91}(1, 1, 1, 1, 1, 1, 2), \quad G_{91}(1, 1, 1, 1, 1, 2, 1), \quad G_{91}(1, 2, 1, 0, 1, 0, 1), \quad G_{91}(2, 0, 1, 1, 0, 1, 1), \quad G_{91}(2, 1, 0, 1, 1, 1, 0), \\
& G_{91}(2, 1, 1, 0, 1, 0, 1).
\end{aligned}
\tag{29}$$

Note that at two-loop order, each family is defined using nine propagators. However, in our case the master integrals are chosen such, that the last two indices are always zero. Thus, we have omitted them in the above list. For convenience we show in Figs. 3 and 4 graphical representations of our one- and two-loop master integrals.

We have cross-checked our expressions against the results given in the ancillary file of [18] and find complete agreement. Note that in [18] the master integrals are expanded to a sufficient order to provide an amplitude to $\mathcal{O}(m_t^2)$. Here, we compute each master integral to a sufficient depth to provide the $gg \rightarrow HH$ amplitude at $\mathcal{O}(m_t^{16})$. We have successfully compared the triangle master integrals to Ref. [48]. In the ancillary file to this paper [23] we provide analytic results for all one- and two-loop planar master integrals discussed here.

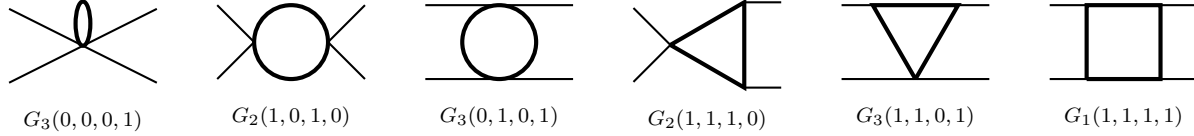


Figure 3: One-loop master integrals. Solid and dashed lines represent massive and massless scalar propagators, respectively. The external (thin) lines are massless. The four master integrals which are not shown are obtained by crossing.

Note that as the integration measure we use $(\mu^2)^{(4-d)/2} e^{\epsilon\gamma_E} d^d k / (i\pi^{d/2})$ where $d = 4 - 2\epsilon$ is the space-time dimension.

B Reducing the dimensionality of Mellin-Barnes integrals

In this appendix, we consider the following two types of Mellin-Barnes integrals:

$$\int_C \frac{dz}{2\pi i} \Gamma \left[\begin{matrix} a_1 - z, a_2 - z, b_1 + z, b_2 + z, b_3 + z \\ c + z \end{matrix} \right], \quad (30)$$

$$\int_C \frac{dz}{2\pi i} \Gamma \left[\begin{matrix} a_1 - z, a_2 - z, b_1 + z, b_2 + z, b_3 + z \\ c + z \end{matrix} \right] \psi(X), \quad (31)$$

with $X = a_1 - z, a_2 - z, b_1 + z, b_2 + z, b_3 + z$ or $c + z$, where the following compact notation has been introduced

$$\Gamma [x_1, \dots, x_n] = \prod_{i=1}^n \Gamma(x_i), \quad \Gamma \left[\begin{matrix} x_1, \dots, x_n \\ y_1, \dots, y_m \end{matrix} \right] = \frac{\Gamma [x_1, \dots, x_n]}{\Gamma [y_1, \dots, y_m]}. \quad (32)$$

Furthermore, we use the compressed notation $a_{12} = a_1 + a_2, b_{123} = b_1 + b_2 + b_3$. In Eqs. (30) and (31) the integration contour C goes from $-i\infty$ to $+i\infty$ and it is assumed that all the poles of $\Gamma [a_1 - z, a_2 - z]$ lie to the right of C and those of $\Gamma [b_1 + z, b_2 + z, b_3 + z]$ to the left of C in the complex z -plane. We also assume

$$\text{Re}(a_i) > 0, \text{Re}(b_j) > 0 \text{ for all } i, j, \quad (33)$$

and choose the contour to be along the imaginary axis. If some of the left poles and the right poles merge, a regularization and a subsequent analytic continuation are required (see the example, discussed below Eq. (42)).

Let us first briefly summarize the known properties of Mellin-Barnes integrals.

- If $c = b_3$, the first Barnes lemma

$$\int_C \frac{dz}{2\pi i} \Gamma [a_1 - z, a_2 - z, b_1 + z, b_2 + z] = \Gamma \left[\begin{matrix} a_1 + b_1, a_1 + b_2, a_2 + b_1, a_2 + b_2 \\ a_1 + a_2 + b_1 + b_2 \end{matrix} \right], \quad (34)$$

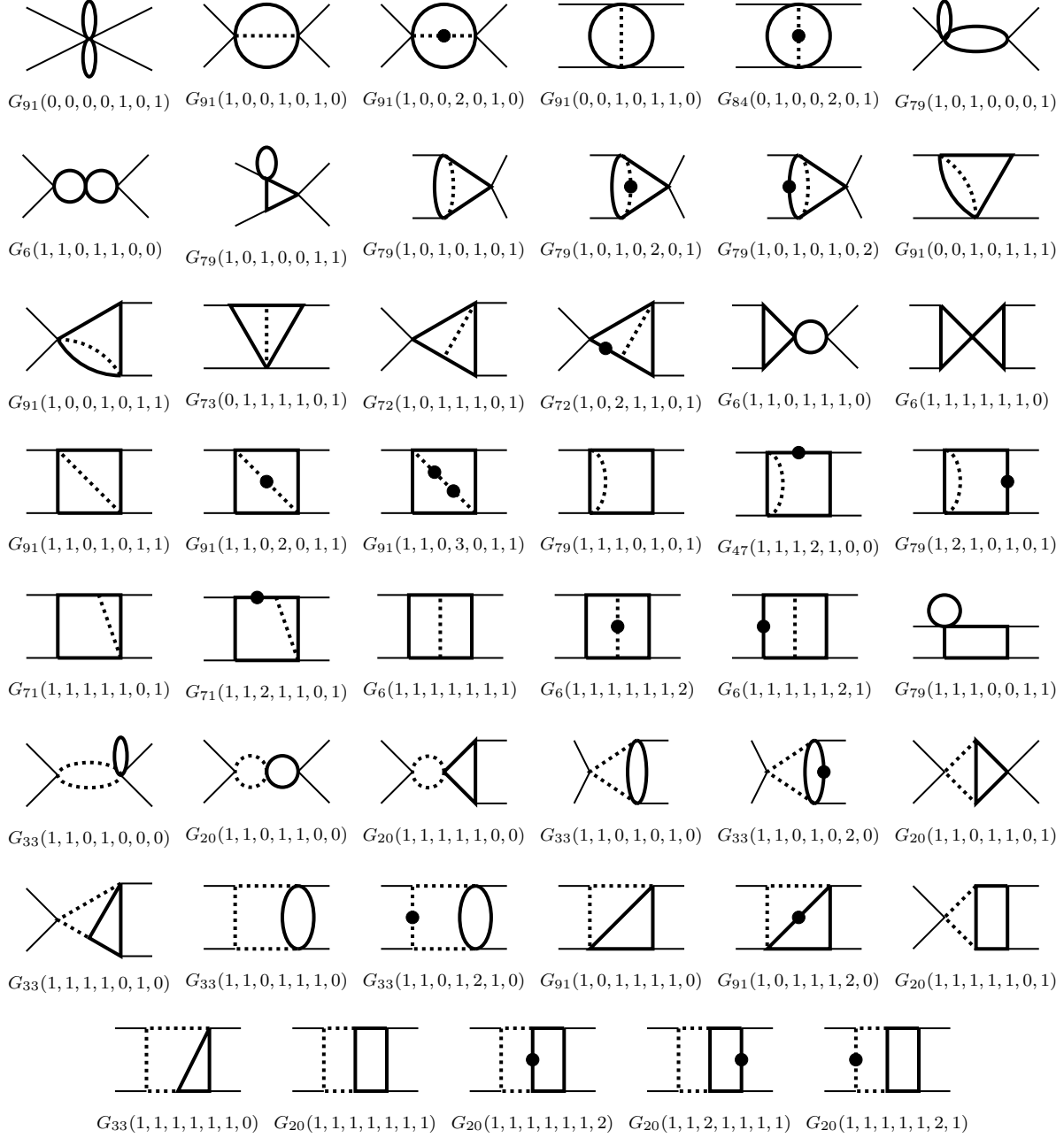


Figure 4: Two-loop planar master integrals. Solid and dashed lines represent massive and massless scalar propagators, respectively. The external (thin) lines are massless. The planar master integrals form (29) which are not shown are obtained by crossing.

can be applied to Eq. (30). By taking a derivative w.r.t. one of the parameters (e.g. a_1) one obtains a solution for Eq. (31).

- If $c = a_{12} + b_{123}$, the second Barnes lemma

$$\begin{aligned} \int_C \frac{dz}{2\pi i} \Gamma \left[\begin{matrix} a_1 - z, a_2 - z, b_1 + z, b_2 + z, b_3 + z \\ a_1 + a_2 + b_1 + b_2 + b_3 + z \end{matrix} \right] \\ = \Gamma \left[\begin{matrix} a_1 + b_1, a_1 + b_2, a_1 + b_3, a_2 + b_1, a_2 + b_2, a_2 + b_3 \\ a_{12} + b_{12}, a_{12} + b_{13}, a_{12} + b_{23} \end{matrix} \right], \end{aligned} \quad (35)$$

can be applied to Eq. (30). However, there is no corresponding expression for Eq. (31); differentiation w.r.t. the parameters a_i, b_j gives relations between expressions which have the form of Eq. (31) with different $X = a_1 - z, a_2 - z, b_1 + z, b_2 + z, b_3 + z, c + z$. The number of independent relations is smaller than the number of possible choices of X . Thus, no analytic result for Eq. (31) can be obtained.

- If $c = a_{12} + b_{123} + 1$ or $c = a_{12} + b_{123} + 2$ the solutions for Eq. (30) are also known [38] and implemented in the package `barnesroutines.m` [45].

In the following we sketch the derivation of a solution for Eq. (30) for the general case, which also yields a solution for Eq. (31) after differentiation w.r.t. one of the parameters.

Based on the assumptions about the relation between a_i, b_j (Eq. (33)), we can express Eq. (30) as

$$\int_C \frac{dz}{2\pi i} \Gamma \left[\begin{matrix} a_1 - z, a_2 - z, b_1 + z, b_2 + z, b_3 + z \\ c + z \end{matrix} \right] = - \sum_{m=0}^{\infty} (\text{Res}_{z=a_1+m} + \text{Res}_{z=a_2+m}), \quad (36)$$

where

$$\begin{aligned} & - \sum_{m=0}^{\infty} \text{Res}_{z=a_1+m} \\ & = \sum_{m=0}^{\infty} (-1)^m \Gamma \left[\begin{matrix} -a_1 + a_2 - m, a_1 + b_1 + m, a_1 + b_2 + m, a_1 + b_3 + m \\ m + 1, a_1 + c + m \end{matrix} \right] \\ & = \Gamma \left[\begin{matrix} -a_1 + a_2, a_1 + b_1, a_1 + b_2, a_1 + b_3 \\ a_1 + c \end{matrix} \right] {}_3F_2 \left(\begin{matrix} a_1 + b_1, a_1 + b_2, a_1 + b_3 \\ 1 + a_1 - a_2, a_1 + c \end{matrix} ; 1 \right). \end{aligned} \quad (37)$$

${}_3F_2$ is the generalized hypergeometric function. The residues at $z = a_2 + m$ are written in a similar manner. At this point the r.h.s. of Eq. (36) contains two ${}_3F_2$. We can transform it into an expression containing only one ${}_3F_2$ using the relation [49],

$$\begin{aligned} {}_3F_2 \left(\begin{matrix} a, b, c \\ d, e \end{matrix} ; 1 \right) & = \Gamma \left[\begin{matrix} 1 - a, -b + c, d, e \\ 1 - a + b, c, -b + d, -b + e \end{matrix} \right] {}_3F_2 \left(\begin{matrix} b, 1 + b - d, 1 + b - e \\ 1 + b - a, 1 + b - c \end{matrix} ; 1 \right) \\ & + \Gamma \left[\begin{matrix} 1 - a, b - c, d, e \\ b, 1 - a + c, -c + d, -c + e \end{matrix} \right] {}_3F_2 \left(\begin{matrix} c, 1 + c - d, 1 + c - e \\ 1 - a + c, 1 - b + c \end{matrix} ; 1 \right). \end{aligned} \quad (38)$$

We additionally apply the relation [49]

$${}_3F_2 \left(\begin{matrix} a, b, c \\ d, e \end{matrix}; 1 \right) = \Gamma \left[\begin{matrix} d, d+e-a-b-c \\ d+e-a-b, d-c \end{matrix} \right] {}_3F_2 \left(\begin{matrix} e-a, e-b, c \\ d+e-a-b, e \end{matrix}; 1 \right), \quad (39)$$

and obtain the following result

$$\begin{aligned} & \int_C \frac{dz}{2\pi i} \Gamma \left[\begin{matrix} a_1 - z, a_2 - z, b_1 + z, b_2 + z, b_3 + z \\ c + z \end{matrix} \right] \\ &= \Gamma \left[\begin{matrix} a_1 + b_1, a_2 + b_1, a_1 + b_2, a_2 + b_2, a_1 + b_3, a_2 + b_3 \\ a_{12} + b_{13}, a_{12} + b_{23}, -b_3 + c \end{matrix} \right] \\ & \times {}_3F_2 \left(\begin{matrix} a_1 + b_3, a_2 + b_3, a_{12} + b_{123} - c \\ a_{12} + b_{13}, a_{12} + b_{23} \end{matrix}; 1 \right). \end{aligned} \quad (40)$$

This is the main result of this appendix. It reduces to the first Barnes lemma for $c = b_j$ and to the second Barnes lemma for $c = a_{12} + b_{123}$.

The l.h.s. of Eq. (40) is symmetric in $a_1 \leftrightarrow a_2$ and $b_1 \leftrightarrow b_2 \leftrightarrow b_3$, however the symmetry among b_j is not obvious on the r.h.s. We can show the symmetry by using the transformation formula of ${}_3F_2$ given in Eq. (39).

In general, the generalized hypergeometric function ${}_3F_2(\{a, b, c\}, \{d, e\}; z)$ converges at $z = 1$ when [50]

$$\operatorname{Re}(d + e - a - b - c) > 0. \quad (41)$$

This condition has to be satisfied when using Eq. (40). If condition (41) is violated we perform an analytic continuation to obtain an expression which converges at $z = 1$. This procedure is well-known [50], so we will not further discuss it here.

The convergence behaviour may change under the replacements $b_1 \leftrightarrow b_2 \leftrightarrow b_3$. By applying the condition (41) to ${}_3F_2$ of Eq. (40), we obtain the condition $\operatorname{Re}(c - b_3) > 0$, which is clearly not symmetric under the replacements $b_1 \leftrightarrow b_2 \leftrightarrow b_3$. Thus the convergent domain, in terms of the space spanned by a_1, a_2, b_1, b_2, b_3 , can differ from expression to expression.

As an example, let us consider the integral

$$\int_C \frac{dz_1}{2\pi i} \Gamma[-z_1, -z_1 - z_2, z_1, 1 + z_1 + z_2] \psi(1 + z_1). \quad (42)$$

In this case, the right-most left-pole at $z_1 = 0$ merges with the left-most right-pole. To separate the poles we introduce a regularization parameter $\delta > 0$ as $\Gamma(z_1) \rightarrow \Gamma(\delta + z_1)$ assuming

$$-1 < -\delta < \operatorname{Re}(z_1) < \operatorname{Re}(z_2) < 0 \quad (43)$$

and analytically continue $\delta \rightarrow 0$ later. By applying the replacements

$$\{a_1 \rightarrow 0, a_2 \rightarrow -z_2, b_1 \rightarrow 1, b_2 \rightarrow \delta, b_3 \rightarrow 1 + z_2, c \rightarrow 1 + \tilde{c}, X \rightarrow 1 + z_1\} \quad (44)$$

to Eq. (40), we have

$$\begin{aligned} & \int_C \frac{dz_1}{2\pi i} \Gamma \left[\begin{matrix} -z_1, -z_1 - z_2, 1 + z_1, \delta + z_1, 1 + z_1 + z_2 \\ 1 + \tilde{c} + z_1 \end{matrix} \right] \\ &= \frac{1}{\delta - \tilde{c}} \left(\Gamma \left[\begin{matrix} \delta, 1 - z_2, z_2 \\ \tilde{c} \end{matrix} \right] - \Gamma \left[\begin{matrix} \delta - z_2, 1 - z_2, z_2 \\ \tilde{c} - z_2 \end{matrix} \right] \right), \end{aligned} \quad (45)$$

where the Gauss summation formula

$${}_3F_2 \left(\begin{matrix} a, b, d \\ c, d \end{matrix}; 1 \right) = {}_2F_1 \left(\begin{matrix} a, b \\ c \end{matrix}; 1 \right) = \Gamma \left[\begin{matrix} c - a - b, c \\ c - a, c - b \end{matrix} \right] \quad (46)$$

has been used. After differentiating w.r.t. \tilde{c} and setting $\tilde{c} \rightarrow 0$, we find

$$\begin{aligned} & \int_C \frac{dz_1}{2\pi i} \Gamma [-z_1, -z_1 - z_2, \delta + z_1, 1 + z_1 + z_2] \psi(1 + z_1) \\ &= -\frac{\gamma_E \Gamma[1 + z_2, -z_2]}{\delta} + \frac{\Gamma[1 + z_2, -z_2]}{2} (\gamma_E^2 + \zeta_2 + \psi(-z_2)^2 - \psi'(-z_2)) + \mathcal{O}(\delta). \end{aligned} \quad (47)$$

Finally we can analytically continue $\delta \rightarrow 0$ as mentioned above; the r.h.s. becomes

$$\begin{aligned} & \int_C \frac{dz_1}{2\pi i} \Gamma [-z_1, -z_1 - z_2, \delta + z_1, 1 + z_1 + z_2] \psi(1 + z_1) \\ &= \int_C \frac{dz_1}{2\pi i} \Gamma [-z_1, -z_1 - z_2, z_1, 1 + z_1 + z_2] \psi(1 + z_1) \\ &\quad - \frac{\gamma_E \Gamma[1 + z_2, -z_2]}{\delta} + \Gamma[1 + z_2, -z_2] (\gamma_E^2 - \zeta_2 - \gamma_E \psi(-z_2) + \gamma_E \psi(1 + z_2)) + \mathcal{O}(\delta) \end{aligned} \quad (48)$$

and therefore

$$\begin{aligned} & \int_C \frac{dz_1}{2\pi i} \Gamma [-z_1, -z_1 - z_2, z_1, 1 + z_1 + z_2] \psi(1 + z_1) \\ &= \frac{\Gamma[1 + z_2, -z_2]}{2} \left[-\gamma_E^2 + \frac{\pi^2}{2} + 2\gamma_E \psi(-z_2) + \psi(-z_2)^2 - 2\gamma_E \psi(1 + z_2) - \psi'(-z_2) \right]. \end{aligned} \quad (49)$$

Throughout this example, z_2 can assume any value satisfying Eq. (43). It can, in particular, be an integration variable. Thus the two dimensional Mellin-Barnes integral of Eq. (42) can be reduced to a one dimensional integral.

References

- [1] E. W. N. Glover and J. J. van der Bij, Nucl. Phys. B **309** (1988) 282.

- [2] T. Plehn, M. Spira and P. M. Zerwas, Nucl. Phys. B **479** (1996) 46 Erratum: [Nucl. Phys. B **531** (1998) 655] [hep-ph/9603205].
- [3] S. Dawson, S. Dittmaier and M. Spira, Phys. Rev. D **58** (1998) 115012 [hep-ph/9805244].
- [4] J. Grigo, J. Hoff, K. Melnikov and M. Steinhauser, Nucl. Phys. B **875** (2013) 1 [arXiv:1305.7340 [hep-ph]].
- [5] G. Degrassi, P. P. Giardino and R. Grber, Eur. Phys. J. C **76** (2016) no.7, 411 [arXiv:1603.00385 [hep-ph]].
- [6] F. Maltoni, E. Vryonidou and M. Zaro, JHEP **1411** (2014) 079 [arXiv:1408.6542 [hep-ph]].
- [7] D. de Florian and J. Mazzitelli, Phys. Lett. B **724** (2013) 306 [arXiv:1305.5206 [hep-ph]].
- [8] D. de Florian and J. Mazzitelli, Phys. Rev. Lett. **111** (2013) 201801 [arXiv:1309.6594 [hep-ph]].
- [9] J. Grigo, K. Melnikov and M. Steinhauser, Nucl. Phys. B **888** (2014) 17 [arXiv:1408.2422 [hep-ph]].
- [10] J. Grigo, J. Hoff and M. Steinhauser, Nucl. Phys. B **900** (2015) 412 [arXiv:1508.00909 [hep-ph]].
- [11] D. Y. Shao, C. S. Li, H. T. Li and J. Wang, JHEP **1307** (2013) 169 [arXiv:1301.1245 [hep-ph]].
- [12] D. de Florian and J. Mazzitelli, JHEP **1509** (2015) 053 [arXiv:1505.07122 [hep-ph]].
- [13] G. Ferrera and J. Pires, JHEP **1702** (2017) 139 [arXiv:1609.01691 [hep-ph]].
- [14] D. de Florian, M. Grazzini, C. Hanga, S. Kallweit, J. M. Lindert, P. Maierhofer, J. Mazzitelli and D. Rathlev, JHEP **1609** (2016) 151 [arXiv:1606.09519 [hep-ph]].
- [15] S. Borowka, N. Greiner, G. Heinrich, S. P. Jones, M. Kerner, J. Schlenk and T. Zirke, JHEP **1610** (2016) 107 [arXiv:1608.04798 [hep-ph]].
- [16] S. Borowka, N. Greiner, G. Heinrich, S. P. Jones, M. Kerner, J. Schlenk, U. Schubert and T. Zirke, Phys. Rev. Lett. **117** (2016) no.1, 012001 Erratum: [Phys. Rev. Lett. **117** (2016) no.7, 079901] [arXiv:1604.06447 [hep-ph]].
- [17] G. Heinrich, S. P. Jones, M. Kerner, G. Luisoni and E. Vryonidou, arXiv:1703.09252 [hep-ph].
- [18] K. Kudashkin, K. Melnikov and C. Wever, arXiv:1712.06549 [hep-ph].

- [19] R. Bonciani, V. Del Duca, H. Frellesvig, J. M. Henn, F. Moriello and V. A. Smirnov, JHEP **1612** (2016) 096 [arXiv:1609.06685 [hep-ph]].
- [20] M. Becchetti and R. Bonciani, arXiv:1712.02537 [hep-ph].
- [21] P. Mastrolia, M. Passera, A. Primo and U. Schubert, JHEP **1711** (2017) 198 [arXiv:1709.07435 [hep-ph]].
- [22] R. Gröber, A. Maier and T. Rauh, arXiv:1709.07799 [hep-ph].
- [23] <https://www.ttp.kit.edu/preprints/2018/ttp18-009/>.
- [24] P. Nogueira, J. Comput. Phys. **105** (1993) 279.
- [25] R. Harlander, T. Seidensticker and M. Steinhauser, Phys. Lett. B **426** (1998) 125 [hep-ph/9712228].
- [26] T. Seidensticker, hep-ph/9905298.
- [27] B. Ruijl, T. Ueda and J. Vermaseren, arXiv:1707.06453 [hep-ph].
- [28] A. V. Smirnov, Comput. Phys. Commun. **189** (2015) 182 [arXiv:1408.2372 [hep-ph]].
- [29] R. N. Lee, arXiv:1212.2685 [hep-ph].
- [30] R. N. Lee, J. Phys. Conf. Ser. **523** (2014) 012059 [arXiv:1310.1145 [hep-ph]].
- [31] A. V. Kotikov, Phys. Lett. B **254** (1991) 158.
- [32] T. Gehrmann and E. Remiddi, Nucl. Phys. B **580** (2000) 485 [hep-ph/9912329].
- [33] K. Melnikov, L. Tancredi and C. Wever, Phys. Rev. D **95** (2017) no.5, 054012 [arXiv:1702.00426 [hep-ph]].
- [34] J. M. Henn, Phys. Rev. Lett. **110** (2013) 251601 [arXiv:1304.1806 [hep-th]].
- [35] O. Gituliar and V. Magerya, Comput. Phys. Commun. **219** (2017) 329 [arXiv:1701.04269 [hep-ph]].
- [36] C. Meyer, Comput. Phys. Commun. **222** (2018) 295 [arXiv:1705.06252 [hep-ph]].
- [37] M. Beneke and V. A. Smirnov, Nucl. Phys. B **522** (1998) 321 [hep-ph/9711391].
- [38] V. A. Smirnov, Springer Tracts Mod. Phys. **250** (2012) 1.
- [39] H.R.P. Ferguson and D.H. Bailey, RNR Technical Report, RNR-91-032; H.R.P. Ferguson, D.H. Bailey and S. Arno, NASA Technical Report, NAS-96-005.
- [40] A. V. Smirnov, Comput. Phys. Commun. **204** (2016) 189 [arXiv:1511.03614 [hep-ph]].

- [41] A. Pak and A. Smirnov, *Eur. Phys. J. C* **71** (2011) 1626 [arXiv:1011.4863 [hep-ph]].
- [42] V. A. Smirnov and O. L. Veretin, *Nucl. Phys. B* **566** (2000) 469 [hep-ph/9907385].
- [43] Z. Bern, L. J. Dixon and V. A. Smirnov, *Phys. Rev. D* **72** (2005) 085001 [hep-th/0505205].
- [44] M. Czakon, *Comput. Phys. Commun.* **175** (2006) 559 [hep-ph/0511200].
- [45] D. Kosower, <https://mbtools.hepforge.org/>
- [46] E. Remiddi and J. A. M. Vermaseren, *Int. J. Mod. Phys. A* **15** (2000) 725 [hep-ph/9905237].
- [47] S. Borowka, G. Heinrich, S. Jahn, S. P. Jones, M. Kerner, J. Schlenk and T. Zirke, *Comput. Phys. Commun.* **222** (2018) 313 [arXiv:1703.09692 [hep-ph]].
- [48] C. Anastasiou, S. Beerli, S. Bucherer, A. Daleo and Z. Kunszt, *JHEP* **0701** (2007) 082 [hep-ph/0611236].
- [49] A. P. Prudnikov, Yu. A. Brychkov, O. I. Marichev “Integrals and series, volume 3,” Gordon and Breach Science Publishers (1990).
- [50] L. J. Slater, “Generalized Hypergeometric Functions,” Cambridge University Press, (1966).